Bio-inspired silicon nanospikes fabricated by metal-assisted chemical etching for antibacterial surfaces

Huan Hu, Vince S. Siu, Stacey M. Gifford, Sungcheol Kim, Minhua Lu, Pablo Meyer, and Gustavo A. Stolovitzky

Citation: Appl. Phys. Lett. **111**, 253701 (2017); doi: 10.1063/1.5003817
View online: https://doi.org/10.1063/1.5003817
View Table of Contents: http://aip.scitation.org/toc/apl/111/25
Published by the American Institute of Physics

Bio-inspired silicon nanospikes fabricated by metal-assisted chemical etching for antibacterial surfaces

Huan Hu,[1,a)] Vince S. Siu,[2] Stacey M. Gifford,[3] Sungcheol Kim,[3] Minhua Lu,[2] Pablo Meyer,[3] and Gustavo A. Stolovitzky[3]
[1]*ZJU-UIUC Institute, International Campus, Zhejiang University, Haining, Zhejiang 314400, China*
[2]*Nanobio Group, Micro-systems Technology and Solutions, IBM T.J. Watson Research Center, Yorktown Heights, New York 10598, USA*
[3]*Microsystem Group, IBM T. J. Watson Research Center, Yorktown Heights, New York 10598, USA*

(Received 7 September 2017; accepted 30 November 2017; published online 21 December 2017)

The recently discovered bactericidal properties of nanostructures on wings of insects such as cicadas and dragonflies have inspired the development of similar nanostructured surfaces for antibacterial applications. Since most antibacterial applications require nanostructures covering a considerable amount of area, a practical fabrication method needs to be cost-effective and scalable. However, most reported nanofabrication methods require either expensive equipment or a high temperature process, limiting cost efficiency and scalability. Here, we report a simple, fast, low-cost, and scalable antibacterial surface nanofabrication methodology. Our method is based on metal-assisted chemical etching that only requires etching a single crystal silicon substrate in a mixture of silver nitrate and hydrofluoric acid for several minutes. We experimentally studied the effects of etching time on the morphology of the silicon nanospikes and the bactericidal properties of the resulting surface. We discovered that 6 minutes of etching results in a surface containing silicon nanospikes with optimal geometry. The bactericidal properties of the silicon nanospikes were supported by bacterial plating results, fluorescence images, and scanning electron microscopy images. *Published by AIP Publishing*. https://doi.org/10.1063/1.5003817

Antibacterial surfaces can limit bacterial growth and inhibit infection and therefore are extremely useful in medical implanted medical devices,[1,2] sutures,[3,4] contact lenses,[5] and other medical materials that require sterile surfaces. The common approach for producing an antibacterial surface is to coat or functionalize the surface with a substance that kills bacteria such as metals,[6] chemicals,[7–11] nanoparticles,[12–14] and carbon nanotubes,[15] but the antibacterial surfaces prepared using this approach often lose antibacterial function quickly and often lead to the development of antibiotic properties in bacteria. Recently, scientists discovered that natural surfaces such as wings of insects[16,17] and gecko skins[18] could mechanically kill bacteria by contact solely based on their physical surface structures, showing an alternative strategy for preparing antibacterial surfaces. Recently, several nanofabrication methods have been demonstrated to fabricate these bio-inspired antibacterial surfaces such as reactive ion etching,[19] glancing angle deposition,[20] microwave plasma chemical vapor deposition,[21] and alkaline hydrothermal etching,[22,23] templating from a nanoporous membrane.[24] The first three methods require expensive semiconductor equipment and a vacuum environment. The hydrothermal method usually requires a controlled temperature and pressure conditions and can directly produce nanopatterns on titanium.[23] It normally operates at a temperature above the boiling point of water to generate a saturated vapor pressure. The last templating method requires a predefined nonporous membrane as a mold.

Here, we present fabrication of antibacterial surfaces using the metal-assisted chemical etching method (MacEtch).[25,26] MacEtch has been used in various applications such as photovoltaic cells,[27–31] light emitting diodes,[32] batteries,[33,34] superhydrophobic surfaces,[35–38] and thermoelectric devices.[39] However, no work has been presented on using MacEtch for fabricating antibacterial surfaces. In this paper, we demonstrate the efficient killing of gram-negative bacteria *Escherichia Coli* (*E. Coli*) using silicon nanospike surfaces fabricated by MacEtch. Moreover, we studied how the etching time affects the morphology of the silicon nanospikes and how the morphology affects the bactericidal properties. We found that 6 min MacEtched silicon samples render the best bactericidal property possibly due to the optimal average pitch between nanospikes.

Figure 1(a) illustrates the mechanism of MacEtch that is typically modeled as two steps.[26] First, the reduction of Ag^+ ions injects holes to oxidize silicon at the interface because the electrochemical potential of Ag^+/Ag is more positive than the Fermi energy of the Si substrate. Ag nuclei are formed and then grow into Ag nanoparticles as shown in step (i) in Fig. 1(a). In the second step, the silicon oxide formed at the interface is etched away by hydrofluoric acid [step (ii) in Fig. 1(a)]. As these two steps alternate, the Ag-Si interface propagates down into the silicon substrate forming vertical silicon nanopillars or nanospikes. The final step is to remove Ag dendrites, rendering pristine silicon nanospikes [step (iii) in Fig. 1(a)].

In MacEtch, a mixture of 20 mM silver nitrate and 5 M hydrofluoric was used as etchants.[26] First, a single crystal silicon with the (100) crystal direction was first dipped into Piranha solution for 30 min at 100 °C to remove organic contaminants. Then, we dipped the silicon sample into etchants for MacEtch. Finally, silver nanoparticles deposited on the silicon sample during MacEtch were removed by a mixture

a)Email: huanhu@intl.zju.edu.cn

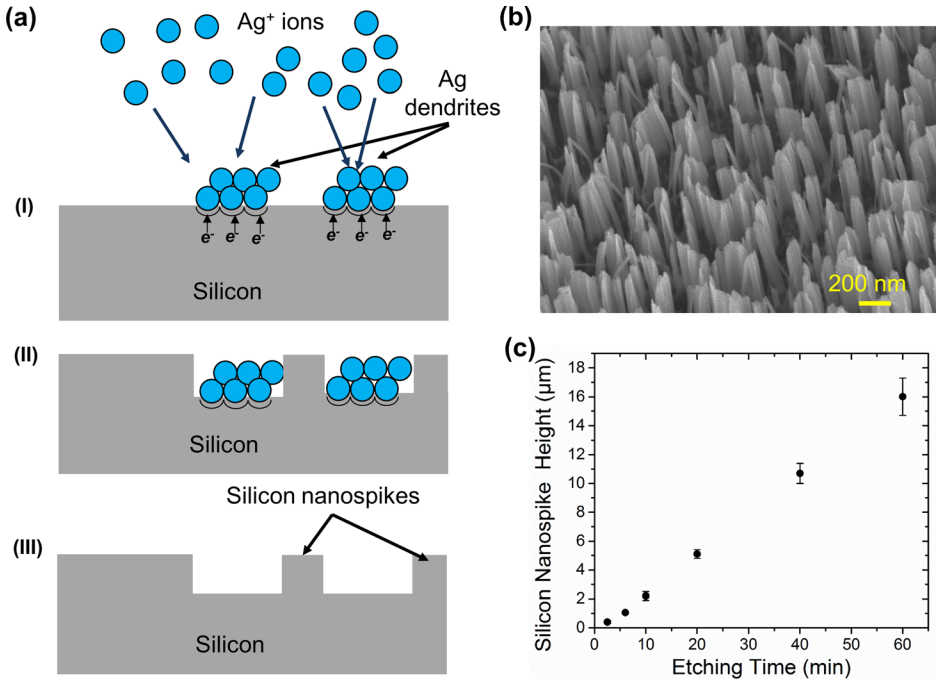

FIG. 1. (a) Schematics showing the mechanism of MacEtch: (i) Ag^{+} ions form silver dendrites on the silicon surface; (ii) silicon underneath the silver dendrites is oxidized and etched by hydrofluoric acid; (ii) remove Ag nanoparticles to render pristine silicon nanospike surface; (b) SEM images of silicon nanospikes produced by 6 min of MacEtch; (c) Measured average heights of silicon nanospikes at different etching time points.

of ammonium hydroxide and hydrogen peroxide with a 3:1 volume ratio to render pristine silicon nanospikes.

After MacEtch, silicon nanospikes were examined in a scanning electron microscope (SEM). Figure 1(b) shows an SEM image of a typical silicon nanospike surface prepared by 6 min MacEtch, wherein randomly distributed nanospikes are clearly seen. Figure 1(c) shows measured heights of silicon nanospikes prepared by different etching durations ranging from 2.5 min to 60 min, exhibiting a linear dependence. To test the bactericidal activity of the silicon nanospike surfaces meaning how efficiently the silicon nanospikes sample can kill bacteria in a liquid suspension, a protocol as illustrated in Fig. S1 (supplementary material) was used. See supplementary material for details.

Many parameters of nanostructures can affect antibacterial properties such as the size, shape, density, rigidity, and surface chemistry.[40] Among all the factors, three crucial parameters of the nanospike topography determine the bactericidal efficiency: the diameter of the spikes, the spacing between the spikes, and the height of the spikes. The diameter of the nanospikes produced by MacEtch is generally intrinsic to the process and is normally distributed between 20 and 300 nm with an average diameter of around 100 nm,[41] agreeing well with nanospikes found on wings of Cicadas. The height of the spikes can be easily controlled by adjusting the etching durations (biology nanospikes 200 nm to 1 μm). The pitch between the silicon nanospikes remains much less studied since most applications of MacEtch use dense nanowire geometry for light trapping in photovoltaic applications.[28]

We experimentally studied the pitch dependence on the etching durations. We discovered that 6 min MacEtch produced silicon nanospike geometry most similar to the biological nanospikes in dragonfly in terms of both the height and pitch. 3 samples prepared at 2.5, 6, and 10 min of MacEtch were examined in SEM as shown in Fig. 2. The left column of images was taken at 30 000× magnification, and the right columns were taken at 100 000× magnification, providing more detailed morphologies. ImageJ was used to derive the average pitch of spikes and the height from 20 random measurements based on captured SEM images. At 2.5 min of MacEtch as shown in Figs. 2(a) and 2(b), a large portion of the silicon surface is not yet etched into the nanospike morphology. As a result, spikes are formed in a low density with the average pitch between spikes measured to be around 400 nm. As etching time increases to 6 min as shown in Figs. 2(c) and 2(d), more nanospikes are formed, and spike density increases. As a result, the average pitch between spikes decreases to about 220 nm. As etching time increases to 10 min as shown in Figs. 2(e) and 2(f), nanospikes are more than 2 μm tall and more likely to form spike bundles due to capillary force during sample drying.[42,43] As a result of bundle formation, the average pitch increases to about 800 nm.

Figure 3 shows the bactericidal test result of three MacEtch samples and a smooth silicon control sample. The control sample results in the maximum number of surviving bacteria since it lacks the antibacterial properties. The number of survived bacteria for the control increases at 3 and 24 h due to remaining nutrients and starts to decrease at 30 h incubation time due to the depletion of available nutrients as also seen in other bactericidal test reports.[19] The 2.5 min MacEtched sample shows similar trends to the control and has a similar amount of colony forming units (CFUs), indicating a non-efficient bacteria killing. In contrast, we do not observe this trend for the 6 min etch and 10 min etch, where the CFU remains constant and lower than control, even when considering the error bars. The 6 min sample remains mostly with the lowest CFU. While all three nanospike samples show significant antibacterial function at 24 h, only the 6 min MacEtch sample still shows significant antibacterial function at both 24 and 30 h. 2.5 and 10 min samples exhibit less bactericidal properties than the 6 min sample as manifested by the much larger bacteria population.

To understand the data quantitatively, we employed a quasi-chemical kinetics model[44,45] widely used for studying cell/bacteria growth and death to fit our data. We found that the comparative death rate of *E. Coli* on the 6 min sample is

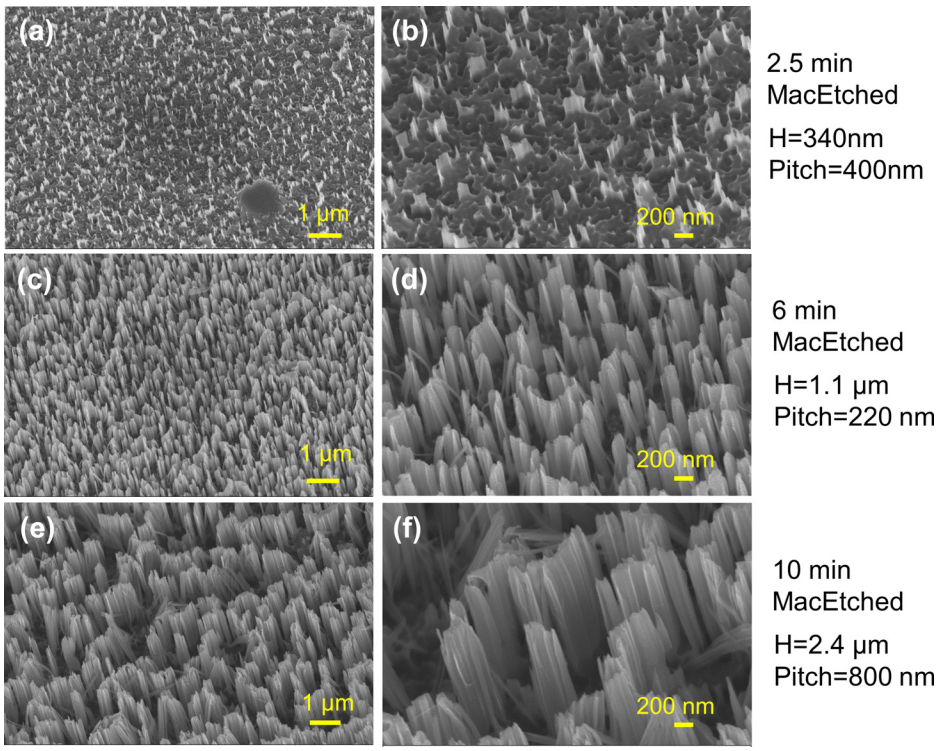

FIG. 2. SEM images of silicon nanospikes formed by MacEtch at 2.5, 6, and 10 min.

two times higher than that of the control sample, further indicating that the silicon nanospikes fabricated by 6 min MacEtch exhibit bactericidal properties. See supplementary material for details of modeling.

The reason for 2.5 and 10 minute nanospike samples showing less bactericidal properties might be that the nanospike pitch, defined as center to center distance, is so large that bacteria can sink down between the nanospikes and adhere to the remaining smooth surfaces for survival. There exists an optimal pitch of nanospikes so that bacteria cannot sink down to smooth surfaces between the nanospikes but rather remain on top of them. Also, the bacteria also have limited contact sites when sitting on the nanospike surface. In this situation, large mechanical stresses induce cell deformation and eventually cause fatal damage to the bacteria. We believe that this is the case for the 6 min MacEtch sample. This 220 nm pitch also agrees well with the 130–380 nm range reported by antibacterial studies using nanopatterned polymer surfaces[46] and the 170 nm pitch of nanopillars on wings of Cicada.[16]

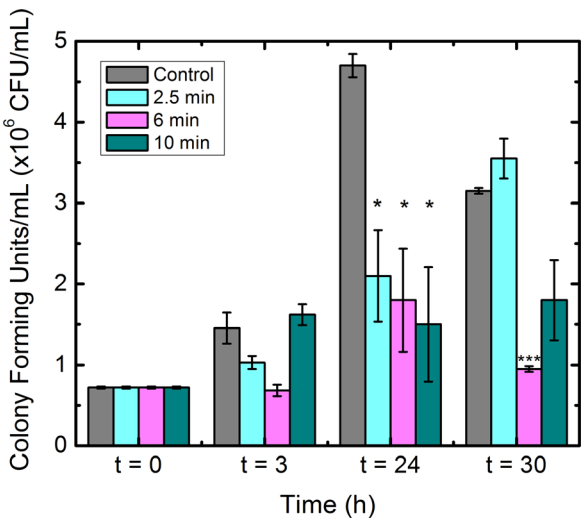

FIG. 3. *E. Coli* bacterial growth is reduced in the presence of 6 min MacEtch samples. Culture samples were plated and colonies were quantified at 0, 3, 24, and 30 h. The plot shows the number of colony forming units (CFU)/mL in culture. *$p < 0.05$ and ***$p < 0.005$.

After the bactericidal test, we took the control sample and the 6 min MacEtch sample out of the bacteria suspension and let them dry out in air for 24 h. Then, we coat the two samples with the 5 nm thick Ti/Pd film and imaged them under a SEM. The standard cell fixation protocol might be the ideal protocol, but here, air drying is the simplest method without further manipulating the bacteria on the sample for imaging. The fact that we obtained good-quality SEM images of bacteria clearly showing the difference between the survived bacterium and the killed bacterium indicates that this method is sufficient for qualitatively showing the difference.

Figure 4(a) shows a typical surviving bacterium on the smooth silicon sample, showing one bacterium that has just finished duplicating while maintaining its rod-shape, indicating being alive on the smooth silicon sample. Figure 4(b) shows several bacteria killed by the 6 min silicon nanospike sample where bacteria have lost their rod-shape as their cell membranes are ruptured.

Figures 5(a) and 5(b) show an example of a fluorescence image of the stained bacterial suspension incubated 6 h in the presence of the smooth silicon control and the 6 min MacEtch sample, respectively. Living bacteria are tagged with only the green SYTO 9 dye, while non-viable cells are tagged with both SYTO 9 and the red propidium iodide stain. Less live bacteria and less dead bacteria are observed in suspension incubated with the nanospike sample compared to that incubated with the control sample, further proving the bactericidal property of the silicon nanospikes. Figure 5(c)

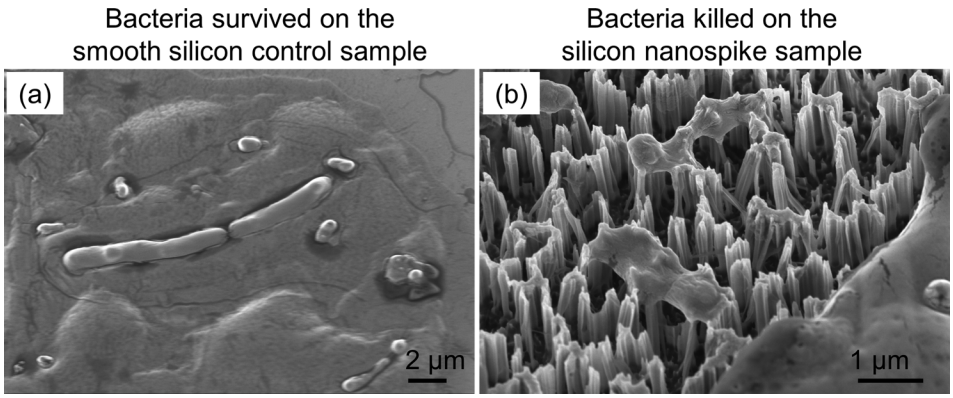

FIG. 4. Scanning electron microscopic image of *E. coli* on a 6 min MacEtch sample surface.

plots the average counts of live bacteria and total bacteria (both live and dead) observed under a fluorescence microscope for 10 random images. Bacterial suspension incubated with the silicon nanospike sample has many less live and dead bacteria. We speculate that this phenomenon is due to more attached bacteria getting killed on the nanospikes and many dead bacteria with disrupted membranes that are not visible under the fluorescence microscope.

The produced silicon nanospikes can be used in two strategies. One strategy is to employ a controlled spalling process[47] that peels off a thin film of silicon containing nanospikes off the substrate. The peeled thin film can be flexible and mounted on non-flat surfaces requiring antibacterial functions. The silicon material offers the advantages of easy integration with electronics, and therefore, more advanced functions such as a smart implant device with antibacterial surfaces can be achieved. Moreover, biocompatible materials such as titanium can be coated on top of the silicon nanostructures if bio-compatibility is a concern. The other strategy is to use the nanostructured silicon surface as a mold to replicate twice, rendering bio-compatible polymer or a plastic material with similar nanostructures for mass-producing antibacterial surfaces.

We present a low-cost and scalable approach for fabricating bio-inspired antibacterial surfaces using MacEtch. We identified the optimal condition of 6 min MacEtch to form the silicon nanospike surface with an average pitch of 220 nm and a tip radius averaged around 100 nm. The 6 min MacEtched nanospike surface can reduce bacterial population by more than half in just 3 h and reduce by more than 3 times the population in 24 h and up to 30 h. Due to its simplicity, low-cost, and scalability, this MacEtch approach is a promising candidate for mass-producing antibacterial surfaces.

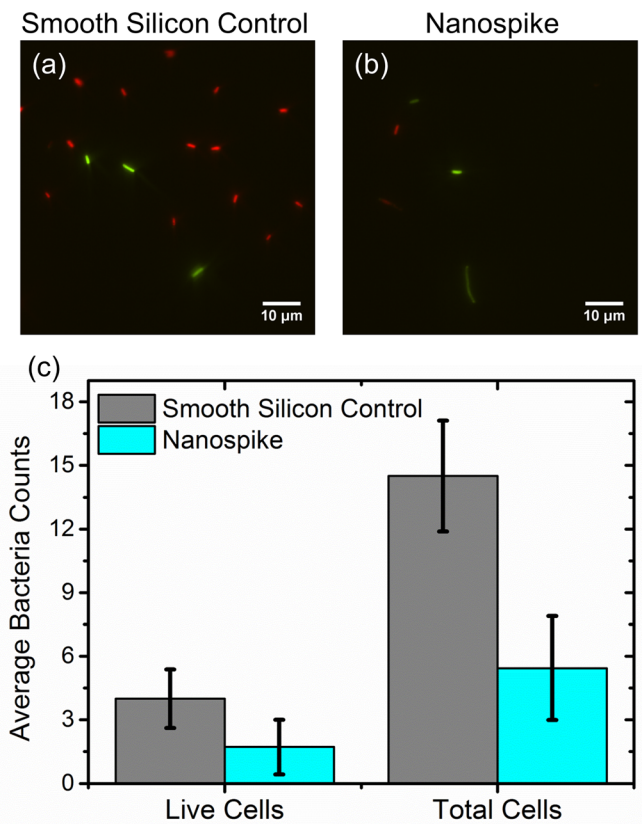

FIG. 5. Fluorescence image of *E. coli* bacteria samples incubated with (a) a smooth silicon control sample and (b) a 6 min MacEtched nanospike sample. (c) The average live bacteria counts and total bacteria counts after incubation with either a smooth or spiked silicon sample across 10 fluorescence images.

See supplementary material for the bactericidal test protocol, the quasi-chemical kinetics model for the cell growth/death with the antibacterial surface, and the fluorescence tagging protocol.

This work was supported by internal IBM research funding. The authors thank Dr. Vikhram Swaminathan for help with the metal-assisted chemical etching experimental design.

[1]K. Vasilev, J. Cook, and H. J. Griesser, "Antibacterial surfaces for biomedical devices," Expert Rev. Med. Devices **6**, 553–567 (2009).
[2]L. Zhao, P. K. Chu, Y. Zhang, and Z. Wu, "Antibacterial coatings on titanium implants," J. Biomed. Mater. Res., Part B **91B**, 470–480 (2009).
[3]X. Chen, D. Hou, L. Wang, Q. Zhang, J. Zou, and G. Sun, "Antibacterial surgical silk sutures using a high-performance slow-release carrier coating system," ACS Appl. Mater. Interfaces **7**, 22394–22403 (2015).
[4]S. Miyake, S. Ito, Y. Oka, J. Kambayashi, and K. Okahara, "Antibacterial vascular prosthesis and surgical suture," Google Patents (1996).
[5]R. E. Weisbarth, M. M. Gabriel, M. George, J. Rappon, M. Miller, R. Chalmers, and L. Winterton, "Creating antimicrobial surfaces and materials for contact lenses and lens cases," Eye Contact Lens **33**, 426–429 (2007).
[6]E. P. Ivanova, J. Hasan, V. K. Truong, J. Y. Wang, M. Raveggi, C. Fluke, and R. J. Crawford, "The influence of nanoscopically thin silver films on bacterial viability and attachment," Appl. Microbiol. Biotechnol. **91**, 1149–1157 (2011).
[7]B. B. Hsu and A. M. Klibanov, "Light-activated covalent coating of cotton with bactericidal hydrophobic polycations," Biomacromolecules **12**, 6–9 (2011).

[8]T. P. Schaer, S. Stewart, B. B. Hsu, and A. M. Klibanov, "Hydrophobic polycationic coatings that inhibit biofilms and support bone healing during infection," Biomaterials **33**, 1245–1254 (2012).
[9]H. Murata, R. R. Koepsel, K. Matyjaszewski, and A. J. Russell, "Permanent, non-leaching antibacterial surfaces—2: How high density cationic surfaces kill bacterial cells," Biomaterials **28**, 4870–4879 (2007).
[10]S. J. Kim, Y. S. Nam, D. M. Rhee, H.-S. Park, and W. H. Park, "Preparation and characterization of antimicrobial polycarbonate nanofibrous membrane," Eur. Polym. J. **43**, 3146–3152 (2007).
[11]E. H. Jeong, J. Yang, and J. H. Youk, "Preparation of polyurethane cationomer nanofiber mats for use in antimicrobial nanofilter applications," Mater. Lett. **61**, 3991–3994 (2007).
[12]S. Siddhartha, B. Tanmay, R. Arnab, S. Gajendra, P. Ramachandrarao, and D. Debabrata, "Characterization of enhanced antibacterial effects of novel silver nanoparticles," Nanotechnology **18**, 225103 (2007).
[13]C.-N. Lok, C.-M. Ho, R. Chen, Q.-Y. He, W.-Y. Yu, H. Sun, P. K.-H. Tam, J.-F. Chiu, and C.-M. Che, "Silver nanoparticles: Partial oxidation and antibacterial activities," JBIC J. Biol. Inorg. Chem. **12**, 527–534 (2007).
[14]Y. K. Jo, J. H. Seo, B.-H. Choi, B. J. Kim, H. H. Shin, B. H. Hwang, and H. J. Cha, "Surface-independent antibacterial coating using silver nanoparticle-generating engineered mussel glue," ACS Appl. Mater. Interfaces **6**, 20242–20253 (2014).
[15]S. Kang, M. Pinault, L. D. Pfefferle, and M. Elimelech, "Single-walled carbon nanotubes exhibit strong antimicrobial activity," Langmuir **23**, 8670–8673 (2007).
[16]E. P. Ivanova, J. Hasan, H. K. Webb, V. K. Truong, G. S. Watson, J. A. Watson, V. A. Baulin, S. Pogodin, J. Y. Wang, M. J. Tobin *et al.*, "Natural bactericidal surfaces: Mechanical rupture of *Pseudomonas aeruginosa* cells by cicada wings," Small **8**, 2489–2494 (2012).
[17]J. Hasan, H. Webb, V. Truong, S. Pogodin, V. Baulin, G. Watson, J. Watson, R. Crawford, and E. Ivanova, "Selective bactericidal activity of nanopatterned superhydrophobic cicada Psaltoda claripennis wing surfaces," Appl. Microbiol. Biotechnol. **97**, 9257–9262 (2013).
[18]G. S. Watson, D. W. Green, L. Schwarzkopf, X. Li, B. W. Cribb, S. Myhra, and J. A. Watson, "A gecko skin micro/nano structure – A low adhesion, superhydrophobic, anti-wetting, self-cleaning, biocompatible, antibacterial surface," Acta Biomater. **21**, 109–122 (2015).
[19]E. P. Ivanova, J. Hasan, H. K. Webb, G. Gervinskas, S. Juodkazis, V. K. Truong, A. H. F. Wu, R. N. Lamb, V. A. Baulin, G. S. Watson *et al.*, "Bactericidal activity of black silicon," Nat. Commun. **4**, 2838 (2013).
[20]S. Christina, L. Michael, M. Yahya, B. Anna, K. Chinmay, S. B. Pio John, A. S. Thomas, L. Alfred, and K. Manfred, "Structure-related antibacterial activity of a titanium nanostructured surface fabricated by glancing angle sputter deposition," Nanotechnology **25**, 195101 (2014).
[21]L. E. Fisher, Y. Yang, M.-F. Yuen, W. Zhang, A. H. Nobbs, and B. Su, "Bactericidal activity of biomimetic diamond nanocone surfaces," Biointerphases **11**, 011014 (2016).
[22]T. Diu, N. Faruqui, T. Sjöström, B. Lamarre, H. F. Jenkinson, B. Su, and M. G. Ryadnov, "Cicada-inspired cell-instructive nanopatterned arrays," Sci. Rep. **4**, 7122 (2014).
[23]C. M. Bhadra, V. K. Truong, V. T. Pham, M. Al Kobaisi, G. Seniutinas, J. Y. Wang, S. Juodkazis, R. J. Crawford, and E. P. Ivanova, "Antibacterial titanium nano-patterned arrays inspired by dragonfly wings," Sci. Rep. **5**, 16817 (2015).
[24]S. Wu, F. Zuber, J. Brugger, K. Maniura-Weber, and Q. Ren, "Antibacterial Au nanostructured surfaces," Nanoscale **8**, 2620–2625 (2016).
[25]X. Li and P. W. Bohn, "Metal-assisted chemical etching in HF/H_2O_2 produces porous silicon," Appl. Phys. Lett. **77**(16), 2572–2574 (2000).
[26]Z. P. Huang, N. Geyer, P. Werner, J. de Boor, and U. Gosele, "Metal-Assisted chemical etching of silicon: A review," Adv. Mater. **23**, 285–308 (2011).
[27]K. Q. Peng, Y. Xu, Y. Wu, Y. J. Yan, S. T. Lee, and J. Zhu, "Aligned single-crystalline Si nanowire arrays for photovoltaic applications," Small **1**, 1062–1067 (2005).
[28]E. C. Garnett and P. Yang, "Silicon Nanowire radial p−n junction solar cells," J. Am. Chem. Soc. **130**, 9224–9225 (2008).
[29]J. Y. Jung, Z. Guo, S. W. Jee, H. D. Um, K. T. Park, M. S. Hyun, J. M. Yang, and J. H. Lee, "A waferscale Si wire solar cell using radial and bulk p-n junctions," Nanotechnology **21**, 445303 (2010).
[30]K.-Q. Peng, X. Wang, L. Li, X.-L. Wu, and S.-T. Lee, "High-Performance Silicon Nanohole Solar Cells," J. Am. Chem. Soc. **132**, 6872–6873 (2010).
[31]H. Fang, X. Li, S. Song, Y. Xu, and J. Zhu, "Fabrication of slantingly-aligned silicon nanowire arrays for solar cell applications," Nanotechnology **19**, 255703 (2008).
[32]W. Chern, K. Hsu, I. S. Chun, B. P d. Azeredo, N. Ahmed, K.-H. Kim, J-m. Zuo, N. Fang, P. Ferreira, and X. Li, "Nonlithographic patterning and metal-assisted chemical etching for manufacturing of tunable light-emitting silicon nanowire arrays," Nano Lett. **10**, 1582–1588 (2010).
[33]K. Peng, J. Jie, W. Zhang, and S.-T. Lee, "Silicon nanowires for rechargeable lithium-ion battery anodes," Appl. Phys. Lett. **93**, 033105 (2008).
[34]B. M. Bang, H. Kim, H.-K. Song, J. Cho, and S. Park, "Scalable approach to multi-dimensional bulk Si anodes via metal-assisted chemical etching," Energy Environ. Sci. **4**, 5013–5019 (2011).
[35]H. Huan, V. S. Vikhram, F. Mahmoud Reza Zamani, M. Glennys, Y. Junghoon, A. S. Mark, and Z. Likun, "Hierarchically structured re-entrant microstructures for superhydrophobic surfaces with extremely low hysteresis," J. Micromech. Microeng. **24**, 095023 (2014).
[36]M. Cao, X. Song, J. Zhai, J. Wang, and Y. Wang, "Fabrication of Highly Antireflective Silicon Surfaces with Superhydrophobicity," J. Phys. Chem. B **110**, 13072–13075 (2006).
[37]F. Shi, Y. Song, J. Niu, X. Xia, Z. Wang, and X. Zhang, "Facile method to fabricate a large-scale superhydrophobic surface by galvanic cell reaction," Chem. Mater. **18**, 1365–1368 (2006).
[38]Y. Xiu, L. Zhu, D. W. Hess, and C. P. Wong, "Hierarchical Silicon etched structures for controlled hydrophobicity/superhydrophobicity," Nano Lett. **7**, 3388–3393 (2007).
[39]J. P. Feser, J. S. Sadhu, B. P. Azeredo, K. H. Hsu, J. Ma, J. Kim, M. Seong, N. X. Fang, X. L. Li, P. M. Ferreira *et al.*, "Thermal conductivity of silicon nanowire arrays with controlled roughness," J. Appl. Phys. **112**, 114306 (2012).
[40]A. Tripathy, P. Sen, B. Su, and W. H. Briscoe, "Natural and bioinspired nanostructured bactericidal surfaces," Adv. Colloid Interface Sci. **248**, 85–104 (2017).
[41]A. I. Hochbaum, R. Chen, R. D. Delgado, W. Liang, E. C. Garnett, M. Najarian, A. Majumdar, and P. Yang, "Enhanced thermoelectric performance of rough silicon nanowires," Nature **451**, 163–167 (2008).
[42]D. Apurba and C. Subhadra, "Uniform large-scale growth of micropatterned arrays of ZnO nanowires synthesized by a surfactant assisted approach," Nanotechnology **18**, 175607 (2007).
[43]J. J. Hill, K. Haller, B. Gelfand, and K. J. Ziegler, "Eliminating capillary coalescence of nanowire arrays with applied electric fields," ACS Appl. Mater. Interfaces **2**, 1992–1998 (2010).
[44]I. A. Taub, F. E. Feeherry, E. W. Ross, K. Kustin, and C. J. Doona, "A Quasi-chemical kinetics model for the growth and death of staphylococcus aureus in intermediate moisture bread," J. Food Sci. **68**, 2530–2537 (2003).
[45]E. W. Ross, I. A. Taub, C. J. Doona, F. E. Feeherry, and K. Kustin, "The mathematical properties of the quasi-chemical model for microorganism growth–death kinetics in foods," Int. J. Food Microbiol. **99**, 157–171 (2005).
[46]M. N. Dickson, E. I. Liang, L. A. Rodriguez, N. Vollereaux, and A. F. Yee, "Nanopatterned polymer surfaces with bactericidal properties," Biointerphases **10**, 021010 (2015).
[47]W. B. Stephen, F. Keith, L. Paul, S. Davood, A. O. John, and S. Devendra, "Layer transfer by controlled spalling," J. Phys. D: Appl. Phys. **46**, 152002 (2013).